# Characterization of oxide films on 4*H*-SiC epitaxial $(000\bar{1})$ faces by high-energy-resolution photoemission spectroscopy: Comparison between wet and dry oxidation

Yasuto Hijikata,[a] Hiroyuki Yaguchi, and Sadafumi Yoshida
*Department of Electrical and Electronic Systems Engineering, Saitama University, 255 Shimo-Okubo, Sakura-ku, Saitama-shi, Saitama 338-8570, Japan*

Yasutaka Takata
*RIKEN/SPring-8, 1-1-1 Kouto, Mikazuki-cho, Sayo-gun, Hyogo 679-5198, Japan*

Keisuke Kobayashi
*JASRI/SPring-8, 1-1-1 Kouto, Mikazuki-cho, Sayo-gun, Hyogo 679-5148, Japan*

Hiroshi Nohira
*Musashi Institute of Technology, 1-28-1 Tamazutsumi, Setagaya-ku, Tokyo 158-8557, Japan*

Takeo Hattori
*Research Center for Silicon Nano-Science, Advanced Research Laboratories, Musashi Institute of Technology, 8-15-1 Todoroki, Setagaya-ku, Tokyo 158-0082, Japan*

(Received 14 March 2006; accepted 7 July 2006; published online 15 September 2006)

Wet and dry oxide films-4*H*-SiC epitaxial $(000\bar{1})$ C-face interfaces have been characterized by capacitance-voltage (*C-V*) measurements and soft x-ray excited photoemission spectroscopy (SX-PES) and hard x-ray excited photoemission spectroscopy (HX-PES) using synchrotron radiation. The interface state density for wet oxidation is much smaller than that for dry oxidation at any energy level. In the PES measurements, intermediate oxidation states such as $Si^{1+}$ and $Si^{3+}$ were observed. In addition, the areal densities of these states were found to be in a good correspondence with those of the interface states. The reasons for the good electrical characteristics of metal-oxide-semiconductor devices fabricated by wet oxidation are discussed in terms of the depth profiles of oxide films derived from the SX-PES and HX-PES results. © *2006 American Institute of Physics*. [DOI: 10.1063/1.2345471]

## I. INTRODUCTION

The physical properties of silicon carbide (SiC), such as its wide band gap and high-breakdown electric field, are attractive for high-power and high-frequency electronic devices whose specifications are difficult to obtain using Si or GaAs. In addition, SiC can be thermally oxidized, and insulating $SiO_2$ layers, known as superior dielectric films for metal-oxide-semiconductor (MOS) applications, can be grown on it, similar to Si.[1] However, SiC MOS field-effect transistors (FETs), especially for 4*H*-SiC, have problems that need to be resolved before they can be used in practical applications, including their higher on resistances than those predicted from bulk properties. These poor electrical characteristics are likely due to the low channel mobility $\mu_{ch}$ in the inversion layer of SiC MOSFETs; the low $\mu_{ch}$ results from the high interface state density. Therefore, controlling the structure of the oxide-SiC interface is key for improving the performance of SiC MOSFETs.

The oxidation rate of the $(000\bar{1})$ C face is the largest among all hexagonal SiC faces and is approximately ten times larger than that of the SiC (0001) Si face.[2] Hence, utilization of the SiC C face can reduce the processing time needed for the production of SiC MOSFETs. Until several years ago, it had been considered that MOSFETs fabricated on the SiC C face have worse electrical characteristics than those on the SiC Si face.[3] However, it has been reported recently that high-quality epitaxial films have been successfully grown on the 4*H*-SiC C face and achieved $\mu_{ch}$ of over 100 $cm^2/V\,s$ by pyrogenic oxidation technique, i.e., thermal oxidation in a mixture of oxygen and hydrogen ambient, followed by hydrogen annealing.[4–8] These reports have shown that the electrical characteristics of MOSFETs obtained by dry oxidation of the 4*H*-SiC C face are significantly poorer than those obtained by wet oxidation of the 4*H*-SiC C face.[7] In contrast, in the case of the 4*H*-SiC Si face, the difference in the electrical characteristics between wet and dry oxidations is not very significant.[9–11] It is therefore very important to clarify the differences in the interface structures between the wet and dry oxides.

There are many reports on the interfaces between oxide layers and 4*H*-SiC studied by photoemission spectroscopy (PES) to explain the reason for the poor electrical properties. Virojanadara and Johansson[12,13] have investigated dry oxide films on C faces by comparing with those on Si faces. They found that the crystallographic plane is correlated with the intermediate oxidation states localized at the interface. Namely, only the $Si^{2+}$ oxidation states were observed in the case of the C face, and only the $Si^{1+}$ states were observed for

[a]Electronic mail: yasuto@opt.ees.saitama-u.ac.jp

 

the Si face. However, the difference in the electrical properties between the C and Si faces was not discussed. For the comparison between wet and dry oxidations, Kobayashi *et al.*[14] have investigated 6*H*-SiC Si-face-oxide interfaces fabricated by wet oxidation at low temperatures (<1000 °C) and at high temperatures (>1000 °C), and dry oxidation at high temperatures. They found that the interface layer in the case of high-temperature oxidation contains more interface states, attributed to graphitic-carbon-related states, than in the case of low-temperature oxidation. However, the difference in the interface structures between the wet and dry oxides has not yet been clarified. We have recently reported the results of soft x-ray excited (1050 eV) photoemission spectroscopy (SX-PES) using synchrotron radiation ("SPring-8") on dry oxide films on the SiC Si and C faces, and a wet oxide film on the 4*H*-SiC C face.[15] In our report, we showed that the thickness of the compositional transition layer is relevant to the electrical characteristics of MOS devices because the difference in the thicknesses for the three samples is in good correlation to the difference in the areal densities of the interface states.

In this work, in order to clarify the reasons for the large difference in the electrical characteristics of MOS devices with wet and dry oxidations in detail, we have directly compared the interface state density ($D_{it}$) estimated from the capacitance-voltage (*C-V*) measurements with the oxide-SiC C-face interface structure observed by SX-PES measurements by using samples fabricated at the same time. Furthermore, in addition to SX-PES measurements, hard x-ray excited photoemission spectroscopy (HX-PES) measurements have been carried out in order to examine the thicker oxide films than those in SX-PES measurements.

## II. EXPERIMENTS

4*H*-SiC C-face epitaxial films with 8° off-oriented, *n*-type, $N_d - N_a \sim 7 \times 10^{16}$ cm$^{-3}$ were used in this study. After standard RCA cleaning, one SiC substrate was oxidized in pure dry $O_2$ flow at 1100 °C for 10 min, resulting in an oxide thickness of ~20 nm, followed by quenching at room temperature [denoted as sample (DryH)]. Another substrate was oxidized in wet $O_2$ flow ($O_2:H_2O=2:1$) at 900 °C for 60 min and 1100 °C for 5 min, resulting in the same oxide thickness as sample (DryH), also followed by quenching [denoted as samples (WetL) and (WetH), respectively]. MOS capacitors for *C-V* measurements were fabricated by thermal evaporation of aluminum through a shadow mask and had a gate-electrode diameter of 0.5 mm. *C-V* measurements were performed using an *LCR* meter (Agilent Corp. 4284A) with a 1 MHz driving frequency, time constant of 10 s, and at room temperature. The values of $D_{it}$ were estimated by the Terman method.[16]

The electron escape depths of Si 2*p* photoelectrons in $SiO_2$ excited by 1050 eV photons and Si 1*s* photoelectrons excited by 4950 eV photons are 2.86 and 8.60 nm, respectively, obtained by considering the dependence of the electron escape depth on the kinetic energy of the electrons. In contrast to the oxide thickness of the specimen for the *C-V* measurements (>10 nm), the thickness used for the PES measurements should be on the order of the escape depth (a few nanometers) to observe the interface structure. Accordingly, all the oxide films were etched by buffered HF to around 1.4 and 5.2 nm for the SX-PES and HX-PES studies, respectively. The thicknesses of the samples used in the PES measurements were measured by a spectroscopic ellipsometer. We have shown that the structures of the interface layers of thick oxide films are different from those of ultrathin oxide films at the initial oxidation stage based on investigations on oxide-4*H*-SiC interfaces using oxide film with varying thickness (so-called slope-shaped oxide films[17]) as well as oxidation time dependence of oxide-6*H*-SiC interface structures by spectroscopic ellipsometry.[18,19] Therefore, the correlation between PES and electrical measurements can be made only when we use thin oxide films fabricated by etching thick oxide films, and cannot be made using ultrathin oxide films at the initial oxidation stage. This is the reason why we do not use ultrathin oxide films but use etched ones for PES measurements. Since the electrical properties of 4*H*-SiC MOS structures are very sensitive to the postoxidation-process conditions,[20] thermal cleaning in vacuum was not done before the PES measurements in order to avoid changing the interface structures.

The SX- and HX-PES measurements were performed using synchrotron radiation (undulator beamlines BL27US and BL47XU of SPring-8, respectively) as a light source and a hemispherical analyzer (Gammadata Scienta SES2002) as an electron analyzer. The photon energies of 4950 and 1050 eV were used for the hard x-ray excited and the soft x-ray excited core level studies, respectively. The normalized energy resolution $\Delta E/E$ in the measurements was less than $2 \times 10^{-4}$.

## III. RESULTS AND DISCUSSION

### A. Energy distribution of interface states

Figure 1 shows the *C-V* curves (a) and $D_{it}$ distributions (b) for the samples (DryH), (WetL), and (WetH). As seen in Fig. 1(a), sample (DryH) shows the large positive shift of flatband voltage, attributed to the high density of negative charges, resulting in the missing accumulation region of the *C-V* characteristic. In the previous report,[20] we have pointed out that nonbonding oxygen atoms exist at the interface and are attributed to the interface states at a deep level observed as a large flatband voltage shift. Although the surface orientation of the substrate used here is different from that of the substrate used in Ref. 20 (Si face), the negative charges observed in the case of sample (DryH) are also considered to be attributable to the nonbonding oxygen atoms. Figure 1(b) shows that $D_{it}$ values over the entire range observed in the measurements were reduced dramatically by the use of wet oxidation. Comparing the effect of temperature, the $D_{it}$ values for low temperature are lower than those for high temperature at almost all the energies. These results follow the results obtained by Fukuda *et al.*;[8] however, the $D_{it}$ values in this work are not the same as those obtained by them. This discrepancy likely results from the differences in the postoxidation methods or/and in the characterization methods of $D_{it}$, as reported in Ref. 21.

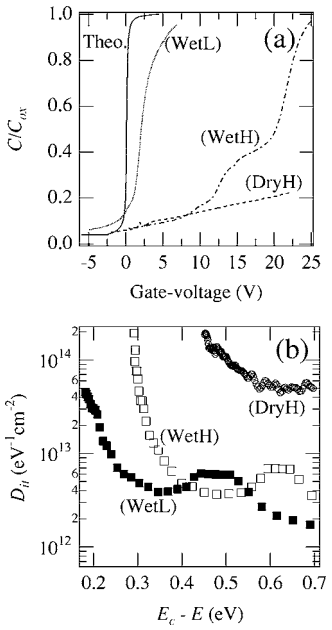


FIG. 1. $D_{it}$ distributions.

### B. C 1*s* photoelectron spectra

The angle-resolved C 1*s* photoemission spectra excited by 1050 eV photons at various photoelectron take-off angles $\theta_e$ for sample (DryH) are shown in Fig. 2. In these measurements, the energy resolution is less than 100 meV. Although we performed the same measurements for sample (WetL), no specific differences compared to sample (DryH) were observed. The figure indicates that a peak originating from a source other than the Si–C bond exists around 284.8 eV. This component peak is considered to originate from the $CH_x$ or C–C bond because its observed binding energy is close to the known values of these bonds.[22] There are many previous reports that have suggested that the high interface state density for oxide-4*H*-SiC systems originates from carbon clusters at the interfaces.[14,23–25] However, as shown in Fig. 2, the intensity of the peak dramatically increases with a decrease in $\theta_e$, which means that the origin of this peak exists at the sample surface rather than the oxide-semiconductor interface. In addition, in our previous work,[17]

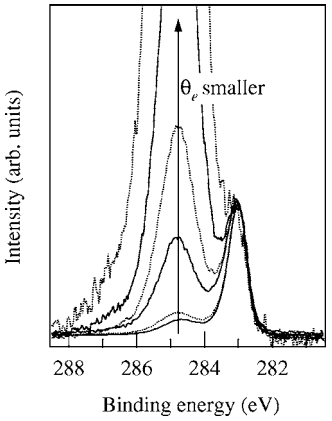


FIG. 2. C 1*s* spectra as a function of the photoelectron take-off angle $\theta_e$ for sample (DryH). The intensity is normalized by the intensity around the SiC peak at another $\theta_e$.

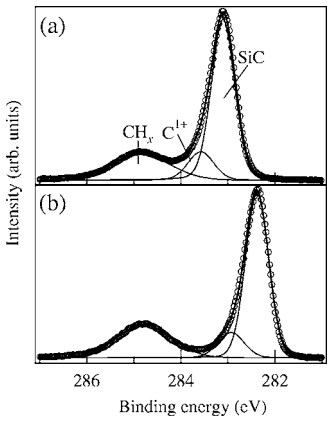


FIG. 3. C 1*s* spectra at $\theta_e$=55°: (a) sample (DryH) and (b) sample (WetL).

we showed that this peak disappears by a prethermal cleaning at 300 °C in vacuum. From these facts, this component peak can be assigned to $CH_x$, i.e., surface contamination. Hereafter, we will use this $CH_x$ peak as a reference for the calibration of binding energy.

Figure 3 shows the C 1*s* photoemission spectra at 55° in $\theta_e$ for the samples (DryH) and (WetL). The measured C 1*s* spectra were decomposed into peaks with superposition of Gaussian and Lorentzian.[26] The component peaks and the sum of all component peaks are shown by thin and thick solid lines, respectively, together with the measured spectra (shown by open circles). As seen in the figure, a shoulder peak is seen at the higher-energy side of the SiC peak. The C 1*s* spectrum obtained from HX-PES (not shown here) also shows this extra peak. This extra peak, denoted as "$C^{1+}$," is thought to originate from $C^{top}-O-Si_3$ ($C^{top}$ denotes the topmost carbon layer in the SiC bulk layer) bonding at the topmost layer of SiC because its binding energy is very close to that of the Si–C bond.

### C. Si 2*p* photoelectron spectra

The angle-resolved Si 2*p* photoemission spectra excited by 1050 eV photons at various $\theta_e$ for the (DryH) and (WetL) samples are shown in Fig. 4. The intensity of the component peaks originating from the oxide layer is larger when $\theta_e$ is smaller, i.e., it is highly surface sensitive.

Figure 5 shows the Si 2*p* photoemission spectra at 55° in $\theta_e$ for the (DryH) and (WetL) samples. The measured spectra were decomposed into peaks with the superposition of

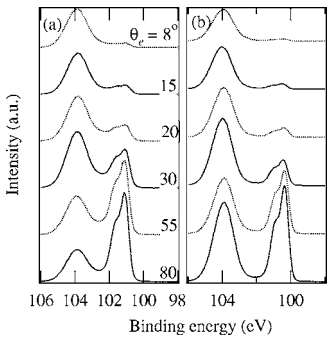


FIG. 4. Si 2*p* spectra at various photoelectron take-off angles $\theta_e$: (a) sample (DryH) and (b) sample (WetL).

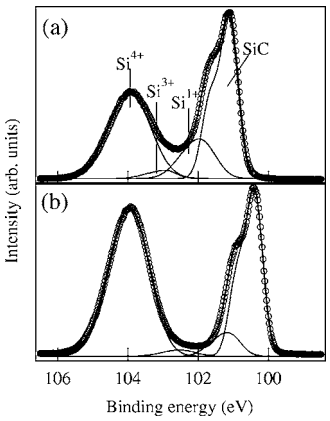


FIG. 5. Si $2p$ spectra at $\theta_e=55°$: (a) sample (DryH) and (b) sample (WetL).

Gaussian and Lorentzian,[27] as mentioned in the analyses of the C $1s$ spectra. Two peaks other than those originating from SiC and $Si^{4+}$ are seen in both cases. The peak around 101 eV is assigned to $Si^{1+}$ oxidation states because of its relative energy from the binding energy of the SiC peak.[15,20,28,29] On the other hand, the peak around 102 eV is assigned to $Si^{3+}$ oxidation states because its relative energy from the binding energy of SiC peak, i.e., 1.9 eV, corresponds to 3/4 the energy separation between SiC and $Si^{4+}$. Also, this relative energy agrees with that reported in Ref. 30. In the case of the Si face, only the $Si^{1+}$ states were reported to be observed as the compositional transition states.[15,20,28,29] Therefore, the $Si^{3+}$ states must be correlated with the carbon polarity face. Based on the fact that these states exist at the interface, they should originate from $C^{top}-Si-O_3$.

### D. Si 1*s* photoelectron spectra

Figure 6 shows 4950 eV photon excited Si $1s$ photoemission spectra at $\theta_e=52°$ for samples (DryH) and (WetL). The energy resolution in the measurements is less than 500 meV. The measured spectra were also decomposed into peaks with superposition of Gaussian and Lorentzian.[31] Similar to the Si $2p$ spectra, compositional transition states such as $Si^{1+}$ and $Si^{3+}$ were observed. Therefore, it is confirmed that the component peaks correlated with these states are not produced by inadequate decomposition of the spectra.

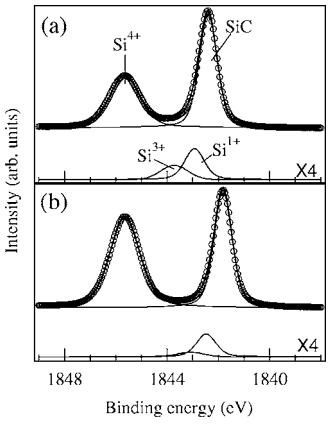


FIG. 6. Si $1s$ spectra at $\theta_e=52°$: (a) sample (DryH) and (b) sample (WetL).

As in the case of Si $2p$, the peak intensities of these states for sample (WetL) are smaller than those for sample (DryH). Nevertheless, the oxide thicknesses of the samples used in HX-PES measurements are about four times larger than those used in SX-PES measurements. This reveals that a small difference in oxide thicknesses does not influence the peak intensity of the compositional transition states.

### E. Depth profile of the bonding structure of the oxide layers

We examined the depth profile of the oxide layers to clarify the cause of the difference in the electrical properties of samples (DryH) and (WetL). The areal density of the compositional transition states, $N_n$, can be estimated from the Si $2p$ photoelectron spectra at a photoelectron take-off angle of 55°, where the effect of elastic scattering can be effectively neglected,[32] by using the following relation:[33,34]

$$\frac{\mathrm{NI}}{\mathrm{NS}}=\frac{N_n}{n_s\lambda_s\sin\theta_e}, \tag{1}$$

where NI/NS represents the intensity of the $Si^{n+}$ peak, i.e., the sum of the $Si^{1+}$ and $Si^{3+}$ peak intensities, normalized by the intensity of the SiC peak, $n_s$ represents the density of the Si atoms in a SiC substrate, and $\lambda_s$ represents the electron escape depth of Si $2p$ photoelectrons excited by 1050 eV photons in the SiC substrate, ~2.0 nm, derived from the value in the case of Mg $K\alpha$ radiation [=2.3 nm (Ref. 17)] by considering the dependence of the electron escape depth on the kinetic energy of the electrons.[35] We used a value of $4.80\times10^{22}$ $cm^{-3}$ for $n_s$. If we assume that the areal density of Si atoms of the $Si^{n+}$ layer equals that of a SiC substrate ($=1.21\times10^{15}$ $cm^{-2}$), then the number of monolayers (MLs) of the compositional transition layer, $M_n$, can be expressed as $N_n/(1.21\times10^{15}\ cm^{-2})$. Assuming that one monolayer corresponds to the Si–C bond length (0.189 nm), the thickness of the compositional transition layer, $d_i$, can be rewritten as $0.189(M_n)$ (nm). The values of $M_n$ and $d_i$ for these samples obtained are listed in Table I. By applying the same analysis for the Si $2p$ spectra to the C $1s$ spectra, the areal density and the thickness of the $C^{1+}$ states, $M_{C1}$ and $d_{C1}$, can be estimated. The values of $M_{C1}$ and $d_{C1}$ obtained are also listed in Table I. In the previous work,[15] we fabricated the sample of SiC Si face by using the same fabrication method as sample (DryH) [denoted as $(\mathrm{DryH})_{\mathrm{Si}}$]. We also estimate the values of $M_n$ and $d_i$ for sample $(\mathrm{DryH})_{\mathrm{Si}}$ and the resulting values are shown in the table. The integrations of the interface state density in the region of $E_c-E=0.2-0.7$ eV, $N_{\mathrm{it}}$, for samples (DryH) and (WetL) as well as $(\mathrm{DryH})_{\mathrm{Si}}$ estimated from Ref. 20 are also listed in Table I. The table indicates that the areal density of the compositional transition states correlates with that of the interface states, while in the case of $C^{1+}$ states, there is no correlation. These results suggest that good electrical characteristics of MOS devices fabricated by wet oxidation of SiC C face can be attributed to the reduction in the areal density of the compositional transition states, and the $C^{1+}$ states may not contribute to the interface states affecting the electrical characteristics of SiC MOS devices.

TABLE I. Areal densities/thicknesses of the compositional transition states and $C^{1+}$ states, $M_n/d_i$ and $M_{C1}/d_{C1}$, respectively, the escape depths of Si $2p$ photoelectrons in the $SiO_2$ layer, $\lambda_o$, the thicknesses of the $SiO_2$ layer, $d_o$, and integration of the interface state density in the region of $E_c-E=0.2-0.7$ eV, $N_{it}$, for samples (DryH) and (WetL), as well as for the dry oxidation film on SiC Si face (Refs. 15 and 20).

| Sample | $M_n/d_i$ (ML/nm) | $M_{C1}/d_{C1}$ (ML/nm) | $\lambda_o$ (nm) | $d_o$ (nm) | $N_{it}$ ($cm^{-2}$) |
|---|---|---|---|---|---|
| (DryH) | 1.64/0.31 | 1.39/0.26 | ··· | 0.76 | $4.1\times10^{13}$ |
| (WetL) | 1.03/0.19 | 1.21/0.23 | 2.57 | 1.12 | $2.7\times10^{12}$ |
| $(DryH)_{Si}$ | 1.47/0.28 | <detection limit | 2.29 | ··· | $1.1\times10^{13}$ |

The escape depth of Si $2p$ photoelectrons in $Si^{4+}$, $\lambda_o$, can be determined from the angle-resolved PES data by using the relation[36]

$$\frac{\mathrm{NI}}{\mathrm{NO}}=\frac{n_i\lambda_i\sin\theta_e[1-\exp(-d_i/\lambda_i\sin\theta_e)]}{n_o\lambda_o\sin\theta_e[\exp(d_o/\lambda_o\sin\theta_e)-1]}, \tag{2}$$

where NO, $n_o$ and $n_i$, $d_o$, and $\lambda_i$ denote the intensity of the $Si^{4+}$ peak, the densities of Si atoms in the $SiO_2$ layer and the compositional transition layer, the thickness of the $SiO_2$ layer, and the electron escape depth of Si $2p$ photoelectrons in the compositional transition layer, respectively. Here, we assumed that $n_o$ was the value for stoichiometric $SiO_2$, and that $n_i=(n_s+n_o)/2$ and $\lambda_i=(\lambda_s+\lambda_o)/2$. We used the value of $2.28\times10^{22}$ $cm^{-3}$ for $n_o$. Figure 7 shows the dependences of NI/NO on $\theta_e$ for samples (DryH) and (WetL). The values of $\lambda_o$ and $d_o$ were determined by least-squares fitting, as shown by the solid curves in the figure. The resulting values of $\lambda_o$ and $d_o$ are listed in Table I. As seen in the figure, the calculated values of NI/NO did not agree well with the measured ones for sample (DryH), especially in the high $\theta_e$ side. As a result, we could not obtain the value of $\lambda_o$ for sample (DryH). This disagreement is likely because its compositional transition layer is not localized at the interface because the calculation model for Eq. (2) is satisfied only when the compositional transition layer is localized at the interface. Although the value of $\lambda_o$ for sample (WetL) is 11% smaller than that for stoichiometric $SiO_2$ (2.86 nm), it is almost the same as that for thermal oxide films on Si (100) faces [2.67 nm (Ref. 36)]. On the other hand, in the case of sample $(DryH)_{Si}$, the value of $\lambda_o$ is considerably smaller compared to that in sample (WetL). As discussed in Sec. III A, a lot of nonbonding oxygen atoms might exist at the interface for sample $(DryH)_{Si}$. Because the nonbonding oxygen atom causes Coulomb scattering against the photoelectron, these nonbonding oxygen atoms therefore can be considered to be one of the causes for the small $\lambda_o$.

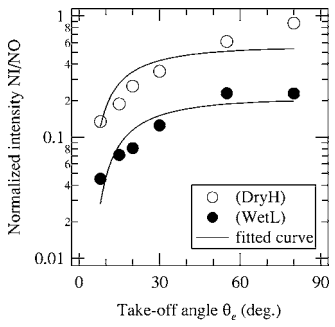


FIG. 7. Dependence of NI/NO on $\theta_e$ for samples (DryH) and (WetL). The solid curves are denoted as fitting curves derived from Eq. (2).

As seen from Figs. 3 and 5 the binding energies of SiC, $C^{1+}$, $Si^{1+}$, and $Si^{3+}$ states for sample (DryH) are around 0.7 eV higher than those for sample (WetL). In the case of the valence-band region,[15] the energy difference of 0.7 eV in the valence-band maximum was also observed. The origin of this binding energy shift can be considered to be the difference in the total thicknesses of the contamination layer and the oxide film, the stress at the interface, or charges trapped at the interface states. Although there is a small difference in these thicknesses between the samples, it cannot account for such a large energy shift. Also, the stress cannot account for the same energy shift at the energy levels in C $1s$, Si $2p$, and the valence-band spectra. The energy shift of 0.7 eV corresponds to the number of interface states per unit area $N_{it}$ of a few $10^{13}$ $cm^{-2}$, which agrees well with that obtained from $C$-$V$ measurements shown in Table I. The binding energy shift therefore can be attributed to the difference in the charges at the interface states. In the Si $1s$ spectra, this energy separation is slightly smaller than 0.7 eV, i.e., ~0.6 eV. This difference can be regarded as the difference in the dielectric constant of the interface layer because the energy difference between the Si $2p$ level and Si $1s$ level depends on the dielectric constant of the interface layer.[37] In our previous report,[20,29] we have pointed out that, in the case of the Si face, the energy difference in the valence-band edge corresponds to $N_{it}$. This correspondence is found to be valid for both the Si and C faces.

Virojanadara and Johansson have reported that other than the SiC component peaks, only the peaks corresponding to the $Si^{2+}$ states in the Si $2p$ spectra and graphitelike-carbon peaks in the C $1s$ spectra were observed in the case of the C face.[12,13] On the contrary, we observed $Si^{1+}$ and $Si^{3+}$ states in the Si $2p$ spectra and $C^{1+}$ states in the C $1s$ spectra. This difference can be explained as follows. In the case of dry oxidation, the difference in binding energies between $Si^{4+}$ and SiC component peaks in the Si $2p$ spectra was found to be about 2.6 eV by Virojanadara and Johansson. As in their case wherein this energy difference is small compared to the widths of these component peaks, the compositional transition state peak is hard to decompose. In our work, although the energy difference in the case of dry oxidation was also 2.6 eV, the energy difference in the case of wet oxidation was expanded to 3.3 eV due to the reduction in the interface trap charges. Hence, we could carry out the decomposition into the $Si^{4+}$, suboxide, and SiC component peaks precisely.

The reason why we observed the shoulder peak in the SiC component at the C 1*s* spectra ($C^{1+}$ state peak) is considered to be the same as in the case of Si 2*p*.

As shown in Table I, the oxide thickness of sample (DryH) estimated from angle-resolved PES, i.e., $d_i+d_o$, is larger than that of sample (WetL). This difference is puzzling because the oxide thicknesses in the two cases estimated from spectroscopic ellipsometry are almost the same. Also, in the case of HX-PES, the intensity ratio of the SiC peak to the peak originating from the oxide layer for sample (DryH) is larger than that for sample (WetL). This difference is thought to be due to the difference in the densities of the compositional transition states between samples (DryH) and (WetL), as follows. In general, a spectroscopic ellipsometer estimates the oxide thickness under the assumption that the refractive index of the oxide layer is equal to that of stoichiometric $SiO_2$. Therefore, when the oxide layer includes a large amount of compositional transition states, the estimated results for oxide thickness have a larger value than that in the case of a smaller amount of compositional transition states because the refractive index of the compositional transition layer is higher than that of stoichiometric $SiO_2$. This interpretation is probably the reason for the difference in the oxide thicknesses between spectroscopic ellipsometry and PES measurements.

The effect of hydrogen termination of the dangling bonds at the interface could be the reason for the improvement in electrical properties for wet oxidation of SiC C face. However, it has been reported that in the case wherein $SiO_2-Si$ structures are exposed to atomic hydrogen, the interface states detected electrically are not reduced well by hydrogen termination of silicon dangling bonds[38] and the interface states relate closely to the compositional transition structure.[34] Therefore, the reduction in the areal density of the compositional transition states for wet oxidation is a promising candidate as the cause for the reduction in the interface states.

## IV. SUMMARY AND CONCLUSIONS

We have studied thermal oxide films on 4*H*-SiC $(000\bar{1})$ epitaxial films by the *C-V* method, and high-resolution SX-PES and HX-PES. The $C^{1+}$, $Si^{1+}$, and $Si^{3+}$ oxidation states were observed at the oxide-SiC interface in both cases of dry and wet oxidations. The bonding structures at the interface were discussed, wherein the $Si^{3+}$ and $C^{1+}$ states are assigned to $C^{top}-Si-O_3$ and $C^{top}-O-Si_3$ bonds at the topmost SiC layer. The relation for the areal density of the interface trap charge between the samples agrees well with that in the areal density of the compositional transition states. These results reveal that the small areal density of the compositional transition states in the case of wet oxidation is attributed to good electrical characteristics of MOS devices on the SiC C face. It is found from angle-resolved PES measurements that the photoelectron escape depth in the $SiO_2$ layer for wet oxidation is almost the same as that for a thermal oxidation film on a Si (100) face.

## ACKNOWLEDGMENTS

The authors would like to thank Dr. Kojima at the National Institute of Advanced Industrial Science and Technology (AIST), Japan, for providing them with SiC epitaxial substrates of the $(000\bar{1})$ face. The synchrotron radiation experiments were performed in the in-vacuum planar undulator beamlines BL27US and BL47XU of SPring-8 with invaluable support from Y. Tamenori, E. Ikenaga, A. Takeuchi, and M. Awaji, and the approval of the Japan Synchrotron Radiation Research Institute as a Nanotechnology Support Project of the Ministry of Education, Culture, Sports, Science and Technology (MEXT). This work is partly supported by an Industrial Technology Research Grant Program (2004-2006) from the New Energy and Industrial Technology Development Organization (NEDO) of Japan and MEXT through a Grant-in-Aid for Scientific Research (A) (No. 15206006).

[1] For example, see S. Yoshida, in *Electric Refractory Materials*, edited by Y. Kumashiro (Dekker, New York, 2000).
[2] A. Gölz, G. Horstmann, E. Stein von Kamienski, and H. Kurz, Inst. Phys. Conf. Ser. **142**, 633 (1996).
[3] K. Fukuda, W. J. Cho, K. Arai, S. Suzuki, J. Senzaki, and T. Tanaka, Appl. Phys. Lett. **77**, 866 (2000).
[4] K. Kojima, T. Suzuki, S. Kuroda, J. Nishio, and K. Arai, Jpn. J. Appl. Phys., Part 2 **42**, L637 (2003).
[5] K. Kojima, H. Okumura, S. Kuroda, and K. Arai, J. Cryst. Growth **269**, 367 (2004).
[6] K. Kojima, H. Okumura, S. Kuroda, K. Arai, A. Ohi, and H. Akinaga, Mater. Sci. Forum **483–485**, 93 (2005).
[7] K. Fukuda, M. Kato, K. Kojima, and J. Senzaki, Appl. Phys. Lett. **84**, 2088 (2004).
[8] K. Fukuda, M. Kato, J. Senzaki, K. Kojima, and T. Suzuki, Mater. Sci. Forum **457–460**, 1417 (2004).
[9] W. Cho, R. Kosugi, J. Senzaki, K. Fukuda, K. Arai, and S. Suzuki, Appl. Phys. Lett. **77**, 2054 (2000).
[10] H. Yano, T. Kimoto, and H. Matsunami, Mater. Sci. Forum **353–356**, 627 (2001).
[11] A. Poggi, F. Moscatelli, A. Scorzoni, G. Marino, R. Nipoti, and M. Sanmartin, Mater. Sci. Forum **527–529**, 979 (2006).
[12] C. Virojanadara and L. I. Johansson, Surf. Sci. **505**, 358 (2002).
[13] C. Virojanadara and L. I. Johansson, Phys. Rev. B **71**, 195335 (2005).
[14] H. Kobayashi, T. Sakurai, M. Takahashi, and Y. Nishioka, Phys. Rev. B **67**, 115305 (2003).
[15] Y. Hijikata, H. Yaguchi, S. Yoshida, Y. Takata, K. Kobayashi, S. Shin, H. Nohira, and T. Hattori, Mater. Sci. Forum **483-485**, 585 (2005).
[16] S. M. Sze, *Physics of Semiconductor Devices*, 2nd ed. (Wiley-Interscience, New York, 1981).
[17] Y. Hijikata, H. Yaguchi, M. Yoshikawa, and S. Yoshida, Appl. Surf. Sci. **184**, 161 (2001).
[18] T. Iida, Y. Tomioka, Y. Hijikata, H. Yaguchi, M. Yoshikawa, Y. Ishida, H. Okumura, and S. Yoshida, Jpn. J. Appl. Phys., Part 2 **39**, L1054 (2000).
[19] T. Iida *et al.*, Jpn. J. Appl. Phys., Part 1 **41**, 800 (2002).
[20] Y. Hijikata, H. Yaguchi, M. Yoshikawa, and S. Yoshida, J. Vac. Sci. Technol. A **23**, 298 (2005).
[21] J. R. LaRoche *et al.*, Electrochem. Solid-State Lett. **7**, G21 (2004).
[22] For example, see J. F. Moulder, W. F. Stickle, P. E. Sobol, and K. D. Bomben, in *Handbook of X-ray Photoelectron Spectroscopy*, edited by J. Chastain, 2nd ed. (Perkin-Elmer, Minnesota, 1992).
[23] V. V. Afanas'ev, A. Stesmans, M. Bassler, G. Pensl, M. J. Schulz, and C. I. Harris, Appl. Phys. Lett. **68**, 2141 (1996).
[24] K. C. Chang, N. T. Nuhfer, L. M. Porter, and Q. Wahab, Appl. Phys. Lett. **77**, 2186 (2000).
[25] W. Lu, L. C. Feldman, Y. Song, S. Dhar, W. E. Collins, W. C. Mitchel, and J. R. Williams, Appl. Phys. Lett. **85**, 3495 (2004).
[26] The parameters selected for the C 1*s* spectra were Lorentzian to Gaussian ratio of 0.1, a Lorentzian width of 0.6 eV, and an asymmetry parameter value of zero. Best spectrum fits were obtained by using Gaussian widths of 0.58, 1.45, and 0.65 eV for SiC, $CH_x$, and $C^{1+}$ components, respectively.

[27]The parameters selected for the Si 2*p* spectra were a spin orbit splitting of 0.55 eV, a branching ratio of 0.50, Lorentzian to Gaussian ratio of zero, and an asymmetry parameter value of zero. Best spectrum fits were obtained by using Gaussian widths of 0.55, 0.80, and 1.23 eV for SiC, suboxide, and $SiO_2$ components, respectively.
[28]L. I. Johansson, C. Virojanadara, Th. Eickhoff, and W. Drube, Surf. Sci. **529**, 515 (2003).
[29]Y. Hijikata, H. Yaguchi, M. Yoshikawa, and S. Yoshida, Mater. Sci. Forum **457–460**, 1341 (2004).
[30]Y. Hoshino, T. Nishimura, T. Yoneda, K. Ogawa, H. Namba, and Y. Kido, Surf. Sci. **505**, 234 (2002).
[31]The parameters selected for the Si 1*s* spectra were Lorentzian to Gaussian ratio of 0.3, a Lorentzian width of 0.9 eV, and an asymmetry parameter value of zero. Best spectrum fits were obtained by using Gaussian widths of 0.82, 1.05, and 1.38 eV for SiC, suboxide, and $SiO_2$ components, respectively.
[32]K. Takahashi, H. Nohira, K. Hirose, and T. Hattori, Appl. Phys. Lett. **83**, 3422 (2003).
[33]T. Suzuki, M. Muto, M. Hara, K. Yamabe, and T. Hattori, Jpn. J. Appl. Phys., Part 1 **25**, 544 (1986).
[34]M. Shioji *et al.*, Appl. Phys. Lett. **84**, 3756 (2004).
[35]M. P. Seah and W. A. Dench, Surf. Interface Anal. **1**, 2 (1979).
[36]H. Nohira *et al.*, Appl. Phys. Lett. **86**, 081911 (2005).
[37]K. Hirose, H. Kitahara, and T. Hattori, Phys. Rev. B **67**, 195313 (2003).
[38]E. Cartier and J. H. Stathis, Microelectron. Eng. **48**, 17 (1999).